Joachim Audet, Mette Vodder Carstensen, Carl C. Hoffmann, Lucile Lavaux, Kirstine Thiemer, Thomas A. Davidson. 2020. Greenhouse gas emissions from urban ponds in Denmark. Inland waters. Vol 10 (3): 373-385

Greenhouse gas emissions from urban ponds in Denmark

Joachim Audet[1], Mette Vodder Carstensen[1], Carl C. Hoffmann[1], Lucile Lavaux[1], Kirstine Thiemer[1,2], Thomas A. Davidson[1]

[1]Department of Bioscience, Aarhus University, Silkeborg, Denmark

[2]Norwegian Institute for Water Research (NIVA), Oslo, Norway

Corresponding author : Joachim Audet, https://orcid.org/0000-0001-5839-8793

E-mail : joau@bios.au.dk

Abstract

Ponds are increasingly recognized as significant sources of greenhouse gases (GHG) emitted to the atmosphere. Concomitant with increasing urbanization, more urban ponds are created, many with the aim of buffering peak runoff flow and improving water quality in downstream waterbodies. However, the impact of urban ponds on GHG emissions is poorly elucidated. In this study, we measured the dissolved concentrations of carbon dioxide (CO_2), methane (CH_4), and nitrous oxide (N_2O) four times over a year in 37 ponds located in the city of Silkeborg, Denmark. The results show that the ponds generally acted as a source of GHG with concentrations of 1938±2208 µg C-CO_2 L^{-1}, 44±198 µg C-CH_4 L^{-1}, and 0.8±1.8 µg N-N_2O L^{-1}. Boosted regression tree models show that vegetation cover, water temperature, and nitrate concentration were the main drivers of CO_2, CH_4, and N_2O concentrations, respectively. Upscaling of the results to Danish national level showed that urban ponds emit about $38x10^9$g CO_2-equivalent per year, which suggests that urban ponds are significant sources of GHG in urban landscapes.

Keywords:

Stormwater; ponds; greenhouse gas; methane; nitrous oxide; carbon dioxide

Introduction

The importance of small waterbodies as hotspots for greenhouse gas (GHG) emissions is increasingly recognized (Holgerson and Raymond 2016; Grinham et al. 2018). Indeed, small waterbodies (<0.1 ha) are reported to be a major source of GHGs accounting for 15% of all carbon dioxide (CO_2) and 40% of all diffusive methane (CH_4) emissions from lakes and ponds, although they comprise only ≈9% of the total area of lentic fresh waters (Holgerson and Raymond 2016). In Queensland, Australia, CH_4 emissions from small artificial waterbodies constituted about 10% of the state's entire land use, land use change, and forestry (LULUCF) sector emissions (Grinham et al. 2018). Nevertheless, the overall contribution of small waterbodies to the total GHG emissions from aquatic ecosystems remains highly uncertain due to i) lack of spatially and temporally representative GHG measurements and ii) poor inventories of natural and human-made waterbodies (Grinham et al. 2018; Koschorreck et al. 2019).

Ponds in urban landscapes have been largely overlooked as sources of GHG, although their number, and therefore spatial extent, is increasing as a consequence of rapid urbanization at the global scale. Hence, in 2018, 55% of the world's population lived in cities and this proportion is projected to reach 68% by 2050 (United Nations 2018). Change in land use, especially increased impervious surfaces due to urbanization, generally results in increased risk of flooding and thus potentially impaired water quality in waterbodies receiving runoff water. To mitigate these risks, ponds are often built to collect stormwater runoff, thus buffering peak events and improving the water quality for receiving waterbodies located further downstream. This is especially relevant in areas of the globe that will face increasing amounts and/or intensity of precipitation. Furthermore, many cities have a stated goal of becoming more sustainable and blue-green infrastructures, including ponds, are set to become more common in urban landscapes. However,

as urban ponds receive nutrients and particles transported in stormwater runoff, they might be important zones for production of GHGs (McPhillips and Walter 2015; D'Acunha and Johnson 2019; Peacock et al. 2019).

In Sweden, Peacock et al. (2019) found that ponds were hotspots for CO_2 and CH_4 emissions in urban areas and recommended a better quantification of their emissions. In addition, most existing studies on GHG emissions from urban ponds have focused on CO_2 and CH_4 emissions, while the emission of the potent GHG nitrous oxide (N_2O) has generally been omitted. However, significant amounts of nitrogen (N) transported to stormwater ponds can be processed here (e.g. denitrified) (Sønderup et al. 2016) which may cause the release of N_2O to the atmosphere (Grover et al. 2013; D'Acunha and Johnson 2019). Hence, it is necessary to assess the significance of urban ponds for GHG emissions.

We measured CO_2, CH_4, and N_2O concentrations in 37 urban ponds in Silkeborg, Denmark, four times during a year. The aim being to quantify and characterise the emissions of GHG from urban ponds with the hypothesis that, despite their limited spatial extent, ponds contribute significantly to the carbon (C) footprint of urban areas.

Material and methods

Study sites

The 37 ponds included in the present study are located in the municipality of Silkeborg, Denmark (Supplementary Table 1). The ponds were selected using aerial photographs. All the ponds, with one exception, were artificial and all were affected by urbanization, i.e. they received urban runoffs from residential areas, industrial areas, parking lots, or roads. The ponds included in this study are intended to remain wet all year round, and some of them are probably influenced by groundwater. The size of the ponds was estimated using aerial photographs and ArcMap version 10.3.1 (ArcGIS, ESRI, Redlands, USA) and varied in size between 135 and 6520 m^2 (Supplementary information). Visual observation revealed that, generally, the maximum depth of the ponds did not exceed 1.5 m. Based on a comparison with aerial photographs from 1954, it appeared that most of the ponds have been built within the last 65 years. Many of the ponds had footpaths around them for recreational purposes. Finally, most ponds hold vegetation, except one with a geotextile bottom which prevents the establishment of rooted macrophytes.

The ponds were sampled four times: August 2018, November 2018, March 2019, and June 2019. The samples were taken between 08.00 and 16.00. The percent cover of the vegetation was estimated visually at every pond and every sampling. The most abundant plant species were identified in June 2019 (Supplementary Table 1).

Sampling methods, chemical analysis, and weather data

Percent oxygen saturation, temperature, and pH in the pond water were recorded *in situ* at about 10 cm depth using a YSI Pro Plus multiparameter meter (YSI, Ohio, USA). Air temperature, atmospheric pressure, and precipitation at the ponds were obtained from the Danish Meteorological Institute (DMI) for the corresponding climatic grid cells (10x10 km grid for precipitation and 20x20 km for daily mean temperature and daily mean atmospheric pressure).

Water samples for nutrient analyses were collected from each pond using a 250 ml polypropylene bottle. Fifty mL subsample were filtered through 0.45 µm filters upon arrival at the laboratory. Both filtered and unfiltered samples were stored in dark at 2°C until analysis, within a week. Filtered samples were used to measure dissolved reactive phosphorus (PO_4^{3-}) and ammonium (NH_4^+) using colorimetric analysis on a Shimadzu 1700 spectrophotometer (Shimadzu Corp., Kyoto, Japan) according to a Danish/European standard method (DS/EN ISO 11732 2005). Total nitrogen (TN) and total organic carbon (TOC) in the unfiltered samples were measured on a TOC-L analyzer equipped with a TNM-L module (Shimadzu, Kyoto, Japan) using standard methods (DS/EN 1484 1997; DS/EN ISO 12260 2003).The method for TN determination was based on oxidation to nitrogen oxides and chemiluminescence detection. TOC determination was based on the non-dispersive infrared detection of the produced CO_2 after a total combustion of the sample. Total phosphorus (TP) in unfiltered samples was analyzed using colorimetric analysis after peroxodisulfate oxidation (DS/EN ISO 6878 2004) on a Shimadzu 1700 spectrophotometer (Shimadzu Corp., Kyoto, Japan). Chloride (Cl^-), nitrate (NO_3^-), and sulphate (SO_4^{2-}) were measured on an ion chromatograph (IC) (DS/EN ISO 10304-1 2007) after filtration at 0.22 µm following sample preparation protocol described in Thermo Scientific (2014).

Greenhouse gas samples and fluxes

Concentrations of CO_2, CH_4, and N_2O in the pond water were measured using the headspace technique (McAuliffe 1971). From all ponds, a 20 mL water sample was collected in the upper 10 cm of the water using a 50 mL polypropylene syringe. Upon sampling, 20 mL N_2 from a gas cylinder were introduced in the syringe to create a headspace and the syringe was vigorously shaken for approx. 60 seconds. Thereafter, the 20 mL headspace was transferred into a 12-ml pre-evacuated borosilicate glass vial (Exetainer, Labco, High Wycombe, UK). The concentrations of CO_2, CH_4, and N_2O were determined using a dual-inlet Agilent 7890 GC system interfaced with a CTC CombiPal autosampler (Agilent, Nærum, Denmark) configured and calibrated with standard gases as described in detail by Petersen et al. (2012). The aqueous concentrations of CO_2, CH_4, and N_2O were calculated from the headspace gas concentrations according to Henry's law and using Henry's constant corrected for water temperature and atmospheric pressure at the sampling time (Weiss 1974; Wiesenburg and Guinasso 1979; Weiss and Price 1980). Because GHG solubility is temperature dependent, all GHG concentrations were standardized to a water temperature of 20°C to ease comparison across seasons. This was done as follow:

$$C_{wat,g,20^\circ} = C_{wat,g,t^\circ} \times \frac{C_{eq,g,20^\circ}}{C_{eq,g,t^\circ}}$$

Where $C_{wat,g,20^\circ}$ is the concentration of a specific gas g dissolved in the water at 20°C, C_{wat,g,t° is the concentration the concentration of a specific gas g dissolved in the water at temperature of sampling t°, $C_{eq,g,20^\circ}$, is the concentration of gas that the water would have at 20°C at equilibrium with the atmosphere assuming atmospheric concentrations of 410, 1.8, and 0.330

ppm for CO_2, CH_4, and N_2O, respectively. $C_{eq,g,t°}$ is the concentration of gas that the water would have at the sampling temperature $t°$ at equilibrium with the atmosphere.

The fluxes of N_2O, CH_4, and CO_2 between the water and the atmosphere were estimated as:

$$f_g = k_g\left(C_{wat,g} - C_{eq,g}\right)$$

where f_g (g m^{-2} h^{-1}) is the flux of a specific gas g, k_g (m h^{-1}) is the gas transfer velocity, and $C_{wat,g} - C_{eq,g}$ (g m^{-3}) is the gradient of concentration between the concentration of gas dissolved in the water ($C_{wat,g}$) and the concentration of gas that the water would have at equilibrium with the atmosphere ($C_{eq,g}$).

$$k_g = k_{600}\left(\frac{Sc_g}{600}\right)^x$$

Sc_g is the Schmidt number (Wanninkhof 1992). We chose x =-2/3 as this factor is used for smooth liquid surface (Deacon 1981). The total greenhouse gas flux was calculated as the sum of CO_2, CH_4, and N_2O after conversion to CO_2-equivalents (CO_2-eq), assuming a global warming potential (GWP) of 34 for CH_4 and 298 for N_2O (IPCC 2013). We assigned a gas transfer velocity k_{600} of 0.36 m d^{-1} as used by Holgerson and Raymond (2016) in their global estimate of CO_2 and CH_4 emissions from small ponds (<0.001 km^2). Annual fluxes were estimated by taking the daily average fluxes for the four sampling days and multiplying by 365 days as there was virtually no ice cover that winter (only 12 days with negative daily mean air temperature over the study period).

An inventory of all the urban ponds in a 10x10 km frame centred on Silkeborg, Denmark (lat. 56.176° long. 9.554°) was made using aerial photographs. To estimate the area of ponds in Denmark, we assumed that the ratio of ponds to urban area in the 10x10 km frame of Silkeborg was representative of the total built-up areas (urban, commercial, industrial, and transport infrastructures) of Denmark. We then applied the mean annual fluxes of GHG from ponds to the total surface of ponds in Denmark to obtain a national estimate.

Statistics

Linear mixed effect models were used to test for differences between the CO_2, CH_4, and N_2O concentrations in the ponds across the four sampling periods as these are particularly suitable to examine the patterns in time series datasets from different sites (Zuur et al. 2009). The mixed models were checked for normality and homogeneity of variance by visual inspection of plots of residuals against fitted values (Zuur et al. 2009). The significance of the models was assessed by comparison with a null-model using the likelihood ratio. To meet the assumption of variance homogeneity in the data when using linear mixed effect models, CO_2, CH_4, and N_2O were transformed using natural-logarithm. The ponds were included as a random effect in the models.

Boosted regression trees (BRT) (De'ath 2007) were used to identify the variables best describing patterns in CO_2, CH_4, and N_2O concentrations in the ponds. We followed the approach of Elith et al. (2008) to find the optimal number of trees. Tree complexity was set at three with a learning rate of 0.001, and with the bag fraction set at 0.7, implying that each individual tree was constructed using 70% of the data, with its predictive ability tested on the remaining 30% (Elith et al. 2008). BRTs are excellent tools for identifying patterns in large complex data sets by using thousands of small trees to find variables that (in this case) best predict the pond concentrations

of CO_2, CH_4 and N_2O. The set of predictor variables consisted of Cl^-, TN, NO_3^-, NH_4^+, TP, PO_4^{3-}, TOC, SO_4^{2-}, oxygen saturation, pH, vegetation cover, and water temperature. Carbon dioxide, CH_4, and N_2O were transformed using natural logarithm prior to the BRT analysis to obtain variance homogeneity (De'ath and Fabricius 2000).

The statistical analyses were performed applying the open source statistical software R version 3.4.4 for Windows (R Development Core Team 2018), employing the package “nlme” and the function “lme” therein (Pinheiro et al. 2012) for the mixed models and the package “gbm” (Greenwel et al. 2019) and the function “gbm.step” for the BRTs (Elith and Leathwick 2017).

Results

The mean air temperature for the period July 2018 to June 2019 was 9.5°C and the sum of the precipitation was 707 mm (Figure 1). The mean (± standard deviation) pond concentrations of dissolved gases across all sites and sampling periods were 1938±2208 µg CO_2-C L^{-1}, 43.5±198 µg CH_4-C L^{-1}, and 0.8±1.8 µg N_2O-N L^{-1} (Table 1). Considering that equilibrium concentrations are about 193 µg C-CO_2 L^{-1}, 0.033 µg C-CH_4 L^{-1}, and 0.27 µg N-N_2O L^{-1} at 20°C, the ponds generally acted as sources of CO_2, CH_4, and N_2O to the atmosphere. Across the sites and sampling periods, the mean values for water temperature, pH, and oxygen were 11.9±7.33°C, 7.6±0.6, and 9.4±2.5 mg O_2 L^{-1}, respectively. Mean pond water concentrations of TN, NO_3^-, and NH_4^+ were 1.07±0.65, 0.35±0.36, and 0.12±0.19 mg N L^{-1}, respectively (Table 1). Mean TP, PO_4^{3-}, and TOC were 0.14±0.19, 0.02±0.04 mg P L^{-1}, and 8.2±7.7 mg L^{-1}, respectively. Mean Cl^- was 50.4±77.8 mg L^{-1}, while mean SO_4^{2-} was 17.4±27.5 mg L^{-1} (Table 1).

Seasonal variations in GHG concentrations and controlling factors

The concentrations of CO_2, CH_4, and N_2O varied across the different sampling periods (Figure 2). Specifically, the CO_2 concentrations in the ponds were significantly lower in March than in August, November, and June (linear mixed models, Supplemental Tables S2 and S3). Methane concentrations in the ponds differed significantly across the four sampling periods, except between November and March when the concentrations also were the lowest (Table 1, Supplemental Tables S2 and S3). The highest CH_4 concentrations were measured in June, which was also the period having the highest water temperature (20°C) (Table 1). The N_2O concentration in the ponds was significantly higher in August compared with November, March, and June (Table 1 and Supplemental Tables S1 and S2). Total nitrogen, NO_3^-, TP, and TOC did

not vary much between the sampling periods (Table 1). Vegetation cover was lowest in March 2019 and highest in June 2019 (Table 1).

Boosted regression trees explained 39, 61, and 46% of the cross validation deviance for CO_2, CH_4, and N_2O, respectively. The BRT helped to identify the variables explaining some of the variation in GHG concentrations. For CO_2 concentrations, the vegetation cover was identified as having the strongest relative influence, explaining 24% of the variation, and higher CO_2 concentrations were found at greater vegetation cover (Figure 3). It was followed by, in order of importance, pH (18%), SO_4^{2-} (12%), oxygen saturation (10%), NH_4 (7%), water temperature (7%), and NO_3^- (6%), while the other variables were below 5%. For CH_4, the five most influential variables were water temperature (31%) followed by NO_3^- (13%), oxygen saturation (9%), PO_4^{3-} (9%), and NH_4^+ (8%) (Figure 4). Increasing water temperature and decreasing NO_3^- seemed connected with an increase in CH_4 concentrations. The pattern of N_2O concentrations was best explained by NO_3^- (37%), water temperature (17%), SO_4^{2-} (11%), oxygen saturation (9%), and vegetation cover (7%), while the other variables were below 5% (Figure 5). Thus, increasing NO_3^- concentrations, water temperatures, and SO_4^{2-} concentrations seemed correlated with greater N_2O concentrations. Plotting the GHG concentrations as a function of the best explanatory variables identified in the BRT models suggests that the relationship between CO_2 and vegetation cover was valid across all seasons (Figure 6a). Although water temperature was identified as the best explanatory variable in the BRT when all sampling periods were considered, concentrations in CH_4 vary largely within each sampling period (Figure 6b). The general trend in greater N_2O concentrations at greater NO_3^- concentration appeared to hold true for every sampling period although it appeared that at similar concentrations of NO_3^-, June and

August samples had higher N_2O concentrations compared to March and November samples (Figure 6c).

Greenhouse gas fluxes and national upscaling

The mean fluxes from the ponds were 628±795 mg C m^{-2} d^{-1}, 15±70 mg C m^{-2} d^{-1}, and, 0.19±0.63 mg N m^{-2} d^{-1} for CO_2, CH_4, and N_2O, respectively. The ponds were always a source of CH_4, but negative fluxes of CO_2 and N_2O occurred, i.e. the ponds acted as a sink for CO_2 (7% of the fluxes) and for N_2O (35% of the fluxes). Although 35% of the N_2O fluxes were negative (52 individual fluxes), they were close to zero as the lowest was -0.06 mg N m^{-2} d^{-1}.

A total of 71 urban ponds were identified in a 10x10 km frame centred on Silkeborg, Denmark. The ponds covered an area of 14.3 ha, while the urban area covered 1760 ha. Hence, the ratio pond:urban area was 0.8%. Assuming that this ratio is representative for urban areas in Denmark (4140 km^2), Danish urban ponds would cover a total surface area of about 34 km^2. Applying the fluxes calculated above to our estimated pond area at national scale amounts to 7.8 $\times 10^9$ g C y^{-1}, 191 $\times 10^6$ g C y^{-1}, 2.4$\times 10^6$ g N y^{-1} for CO_2, CH_4, and N_2O, respectively. Conversion of these fluxes into CO_2-equivalents using a GWP of 34 for CH_4 and 298 for N_2O represents gives a total emission of 38$\times 10^9$ g CO_2-eq y^{-1} from Danish urban ponds. Carbon dioxide constituted 75% of the emissions from the ponds, while CH_4 and N_2O constituted 22% and 3%, respectively.

Discussion

GHG emissions

The 37 ponds surveyed in our study generally acted as sources of GHG to the atmosphere. Our measured concentrations of CO_2 and CH_4 were within the range found in previous studies on urban ponds, comparable with the values (1350 and 26 µg C L^{-1} for CO_2 and CH_4, respectively, median values) recorded in 40 urban ponds in Sweden in late spring (Peacock et al. 2019). The mean CO_2 and CH_4 concentrations (1608 and 91 µg C L^{-1} for CO_2 and CH_4, respectively) found in a global assessment of small natural and artificial ponds (<0.1 ha) were also comparable to our study (Holgerson and Raymond 2016).

In terms of fluxes, our estimates were greater for CO_2 and N_2O but lower for CH_4 than measured in stormwater ponds in Virginia, USA (CO_2, 412 mg C m^{-2} d^{-1}; CH_4, 203 mg C m^{-2} d^{-1}; N_2O, 64 µg N m^{-2} d^{-1}), by Gorsky et al. (2019). However, they only measured summer fluxes and used floating chambers, which means that ebullition events of CH_4 might have been recorded, whereas only diffusive fluxes derived from dissolved concentrations were estimated in our study. Methane fluxes measured from urban ponds in Berlin (88 mg C m^{-2} d^{-1}, diffusion only) were lower than ours (Herrero Ortega et al. 2019). Nitrous oxide emissions measured in stormwater ponds in New York, USA, were also comparable (0.11 mg N m^{-2} d^{-1}) with our values (McPhillips and Walter 2015). However, most studies measuring N_2O have found highly variable emissions rates; thus, peak events up to 1.1 mg N h^{-1} were measured in an urban pond in Melbourne, Australia (Grover et al. 2013), while occasional negative fluxes of N_2O were recorded in an urban pond in Vancouver, Canada (D'Acunha and Johnson 2019).

Seasonal variation

The GHG concentrations in the ponds differed across the sampling period. Carbon dioxide was highest in June and lowest in March, while August and November concentrations were relatively similar despite much colder water temperatures in November. However, in November the vegetation was observed to be decaying, which may partly explain the high CO_2 levels despite the lower temperature. Methane concentrations were the highest in the two warmest sampling occasions, i.e. June and August, which was expected since metabolic rates of CH_4 scale with temperature (Conrad 1996). Nitrous oxide concentrations were relatively similar in November, March, and June but were markedly higher in August. These differences could not be explained by variations in NO_3^- levels as these were relatively constant over the four sampling campaigns. However, average O_2 saturation was lower in August than in the other sampling periods, which may have created favourable conditions for denitrification and the production of N_2O.

Controlling factors

The BRT suggested that the CO_2 concentrations in the ponds were linked to vegetation cover. Photosynthetic activity affects CO_2 concentrations in the pond water, but the higher plant cover would be expected to reduce CO_2 concentrations as seen in other studies (Davidson et al. 2015), which is in apparent contradiction with our findings. However, the pond mesocosms used in the study by Davidson et al. (2015) only hold submerged vegetation, whereas the urban ponds from the present study usually hold emerged species (Supplemental Material Table S1). Therefore, the main source of CO_2 for the vegetation most likely comes from the atmosphere and not from CO_2 dissolved in the water (Sand-Jensen et al. 1992). Furthermore, emerged rooted aquatic macrophytes oxygenate the sediment and provide labile C via their root exudates, which might promote degradation processes and the subsequent release of CO_2 to the water. Another possible explanation for the positive association between CO_2 concentrations and plant cover would be

that allochthonous CO_2 (e.g. from groundwater or runoff) tends to accumulate in ponds having greater plant cover, because of slower degassing to the atmosphere. It has been shown that high vegetation cover by emergent and floating-leaved aquatic plants can reduce turbulence at the surface of the water, resulting in a decreased gradient in CO_2 between air and thus a reduced diffusion of CO_2 (Attermeyer et al. 2016). An alternative hypothesis would be that more particles are trapped in the ponds at greater plant cover and trapped organic matter can, therefore, increase respiration processes (Braskerud 2001). Finally, plants are also a source of C-compounds fuelling respiration processes, especially when decaying in autumn. Carbon dioxide was also strongly correlated with pH in the BRTs, which probably illustrates the link between CO_2 and pH through the carbonate system.

The BRT fitted a positive relationship between CH_4 concentrations and water temperature, which has been demonstrated in several studies (Marotta et al. 2014; van Bergen et al. 2019). However, the reported effect of temperature also reflects seasonal variations and associated changes in ecological composition and structure rather than the sole effect of temperature (Davidson et al. 2015). Hence, it is challenging to disentangle direct and indirect effects of temperature on CH_4 concentration. Oxygen and NO_3^- concentrations were negatively associated to CH_4 concentrations. Methane production usually becomes significant only when the more favourable electron acceptors have been depleted, for example O_2 and NO_3^-. There was a positive relationship between PO_4^{3-} and CH_4 concentrations, which is in line with previous research that has shown an increase in CH_4 emissions with increasing eutrophication (Davidson et al. 2015; Davidson et al. 2018; DelSontro et al. 2018; Beaulieu et al. 2019). The mechanism behind increased CH_4 emissions in eutrophic ponds and lakes is still unclear but might be linked to alteration of ecological structure provoked by excess nutrients, for instance disappearance of

307 macrophytes, formation of algal blooms and production of more labile dissolved organic matter
308 (Davidson et al. 2018; Zhou et al. 2019).

309 Nitrous oxide concentrations increased at higher NO_3^- concentrations, most likely as a result of
310 N_2O produced by denitrification, although other N_2O production pathways such as nitrification
311 cannot be excluded. Warmer water temperature also appeared to increase N_2O concentrations.
312 Water temperature exerts strong control on metabolic processes and at higher water temperature,
313 O_2 will be more rapidly depleted, which is a prerequisite for the creation of anoxic zones in the
314 sediment and for denitrification to occur (Tiedje 1982). Greater SO_4^{2-} was also associated with
315 higher N_2O concentrations. Some studies have shown that the conversion from N_2O to N_2 might
316 be inhibited by sulphide, which is produced by the reduction of SO_4^{2-} (Sørensen et al. 1980).

317 Hydraulic residence time is probably a key variable explaining some of the variation in GHG
318 production in the ponds as it influences the interactions across water, sediment, and biota
319 (Persson and Wittgren 2003). Unfortunately, we did not have any information on the discharge at
320 the ponds, their volume, or the size and land use of the catchment that they drain.

321 *Uncertainties in GHG measurements*

322 In our study, we only measured diffusive emission of CH_4; however, CH_4 ebullition is a major
323 pathway for CH_4 emission. For urban ponds in Berlin, only a fifth of their total CH_4 emission
324 was found to be diffusive (Herrero Ortega et al. 2019), and ebullition constituted 50% of all
325 GHG emissions (in CO_2-eq) in an urban pond in the Netherlands (van Bergen et al. 2019).
326 Consequently, CH_4 emission in our study is underestimated. Stormwater ponds are very
327 hydrologically dynamic and this will affect the production and emission of GHG. Hence, the use
328 of continuous monitoring methods would be beneficial to better constrain GHG estimates. In

addition, the presence of primary producers (e.g., plants, algae) in the ponds will have an effect on the seasonality of production and senescence and on diurnal variation in CO_2. Consequently, continuous monitoring is needed to obtain reliable estimates of CO_2 emissions. Furthermore, the impact of drought and rewetting events might also have a very strong impact on GHG emissions as some studies have shown that drying out of the sediment can lead to substantial emissions of CO_2, and perhaps also of N_2O as highlighted by some studies on streams and ponds (Catalán et al. 2014; Marcé et al. 2019). While it is established that ponds are a hotspot for GHG emissions in urban areas, the true impact of urban ponds on climate is unclear because they might also bury substantial amounts of organic C in their sediments, which may compensate, at least to some extent, for the release of GHGs (Downing et al. 2008; Taylor et al. 2019). However, the burial of organic C in an urban pond in the Netherlands accounted only for 6% of the total emissions of GHG (van Bergen et al. 2019). The effect of pond age on GHG emissions is also unknown; yet, a study by Sønderup et al. (2016) showed that ponds younger than 5 years were the most effective in retaining nutrients, whereas almost no nutrients were retained in ponds older than 10 years.

GHG emissions from urban ponds on a national scale

Assuming that the density of ponds is similar in all urban areas of Denmark, we estimated that the total GHG emissions from Danish urban ponds are 38×10^9 g CO_2-eq y^{-1}. This estimate is equivalent to about 21% of the emissions from waste water treatment and discharge (177×10^9 g CO_2-eq y^{-1}) accounted for in the Danish National Inventories report for the IPCC (Nielsen et al. 2018). Hence, in spite of uncertainties, our study demonstrates that ponds are a significant source of GHG in urban areas. This result is in line with the findings from a recent study on CH_4 emissions from urban waterbodies, including urban ponds, in Berlin, Germany, emphasizing that these emissions ought to be considered in GHG inventories (Herrero Ortega et al. 2019).

Implications for climate adaptations and management

A large number of cities envision becoming “Carbon Neutral” within the next decades (Kennedy and Sgouridis 2011), and therefore we recommend including GHG emissions from urban ponds in their overall GHG assessment. Noteworthy, these emissions have been recently incorporated into IPCC inventories (IPCC 2019). We have shown that emissions of CO_2, CH_4, and N_2O are influenced by water temperature and in a warmer climate, these emissions might therefore further increase. It is, though, unclear whether GHG emissions are more impacted by the direct effect of temperature on metabolic processes or by temperature-induced changes in the nutrient processes and ecological status of ponds (Davidson et al. 2015; Davidson et al. 2018). Hence, temperature driven CH_4 emissions can probably be mitigated by measures aiming at improving the ecological status of ponds. Still, the warming effect might be even stronger in urban areas because of urbanization-driven warming (urban heat island effect), which also increases the water temperature in ponds (Brans et al. 2018). Even though our results indicate that ponds are a significant source of GHG in urban areas, measurement of C-sequestration in these systems is necessary to critically assess their actual C-footprint. High resolution monitoring of GHG emissions would be advantageous to characterize CH_4 ebullition and to capture temporal variations in CO_2. The links identified between GHG emissions and nutrient concentrations might provide opportunities for mitigation by controlling nutrient inputs to urban ponds (Teurlincx et al. 2019). Furthermore, the apparent influence of vegetation on GHG emissions suggests that vegetation management might also have a significant impact on pond GHG budgets (Badiou et al. 2019), although this mitigation option would require further research to clearly characterize how vegetation type, cover, and assemblage affect GHG emissions from urban ponds.

Acknowledgements

The authors would like to thank Marlene Venø Skjærbæk and Dorte Nedergaard for their technical assistance and Anne Mette Poulsen for improving the English language. Silkeborg municipality and Silkeborg Forsyning are acknowledged for granting access to the ponds. JA thanks Mike Peacock for fruitful discussions on the topic of GHG emissions from ponds.

References

Attermeyer K, Flury S, Jayakumar R, Fiener P, Steger K, Arya V, Wilken F, van Geldern R, Premke K. 2016. Invasive floating macrophytes reduce greenhouse gas emissions from a small tropical lake. Sci Rep. 6:20424.

Badiou P, Page B, Ross L. 2019. A comparison of water quality and greenhouse gas emissions in constructed wetlands and conventional retention basins with and without submerged macrophyte management for storm water regulation. Ecol Eng. 127:292-301.

Beaulieu JJ, DelSontro T, Downing JA. 2019. Eutrophication will increase methane emissions from lakes and impoundments during the 21st century. Nat Commun. 10(1):1375.

Brans KI, Engelen JMT, Souffreau C, De Meester L. 2018. Urban hot-tubs: Local urbanization has profound effects on average and extreme temperatures in ponds. Landscape Urban Plann. 176:22-29.

Braskerud BC. 2001. The influence of vegetation on sedimentation and resuspension of soil particles in small constructed wetlands. J Environ Qual. 30(4):1447-1457.

Catalán N, von Schiller D, Marcé R, Koschorreck M, Gomez-Gener L, Obrador B. 2014. Carbon dioxide efflux during the flooding phase of temporary ponds. Limnetica. 33(2):349-360.

Conrad R. 1996. Soil microorganisms as controllers of atmospheric trace gases (H_2, CO, CH_4, OCS, N_2O, and NO). Microbiol Rev. 60(4):609-640.

D'Acunha B, Johnson MS. 2019. Water quality and greenhouse gas fluxes for stormwater detained in a constructed wetland. J Environ Manage. 231:1232-1240.

Davidson TA, Audet J, Jeppesen E, Landkildehus F, Lauridsen TL, Søndergaard M, Syväranta J. 2018. Synergy between nutrients and warming enhances methane ebullition from experimental lakes. Nat Clim Change. 8(2):156-160.

403 Davidson TA, Audet J, Svenning J-C, Lauridsen TL, Søndergaard M, Landkildehus F, Larsen
404 SE, Jeppesen E. 2015. Eutrophication effects on greenhouse gas fluxes from shallow-lake
405 mesocosms override those of climate warming. Global Change Biol. 21(12):4449-4463.
406 De'ath G. 2007. Boosted trees for ecological modeling and prediction. Ecology. 88(1):243-251.
407 De'ath G, Fabricius KE. 2000. Classification and regression trees: A powerful yet simple
408 technique for ecological data analysis. Ecology. 81(11):3178-3192.
409 Deacon EL. 1981. Sea-air gas transfer: The wind speed dependence. Boundary-Layer Meteorol.
410 21(1):31-37.
411 DelSontro T, Beaulieu JJ, Downing JA. 2018. Greenhouse gas emissions from lakes and
412 impoundments: Upscaling in the face of global change. Limnol Oceanogr Lett. 3(3):64-75.
413 Downing JA, Cole JJ, Middelburg JJ, Striegl RG, Duarte CM, Kortelainen P, Prairie YT, Laube
414 KA. 2008. Sediment organic carbon burial in agriculturally eutrophic impoundments over the
415 last century. Global Biogeochem Cy. 22(1).
416 DS/EN 1484. 1997. Water analysis – Guidelines for the determination of total organic carbon
417 (TOC) and dissolved organic carbon (DOC).
418 DS/EN ISO 6878. 2004. Water quality - Determination of phosphorus - Ammonium molybdate
419 spectrometric method.
420 DS/EN ISO 10304-1. 2007. Water quality – Determination of dissolved anions by liquid
421 chromatography of ions – Part 1: determination of bromide, chloride, fluoride, nitrate, nitrite,
422 phosphate, and sulfate.
423 DS/EN ISO 11732. 2005. Determination of ammonium nitrogen - Method by flow analysis
424 (CFA and FIA) and spectrometric detection.

425 DS/EN ISO 12260. 2003. Water quality – Determination of nitrogen – Determination of bound
426 nitrogen (TNb) following oxidation to nitrogen oxides.
427 Elith J, Leathwick J. 2017. Boosted Regression Trees for ecological modeling. [accessed 2019
428 Nov 12]. https://cran.r-project.org/web/packages/dismo/vignettes/brt.pdf.
429 Elith J, Leathwick JR, Hastie T. 2008. A working guide to boosted regression trees. J Anim Ecol.
430 77(4):802-813.
431 Gorsky AL, Racanelli GA, Belvin AC, Chambers RM. 2019. Greenhouse gas flux from
432 stormwater ponds in southeastern Virginia (USA). Anthropocene.100218.
433 Greenwel B, Boehmke B, Cunningham J, GBM Developers. 2019. gbm: Generalized Boosted
434 Regression Models R package version 2.1.5. https://CRAN.R-project.org/package=gbm.
435 Grinham A, Albert S, Deering N, Dunbabin M, Bastviken D, Sherman B, Lovelock CE, Evans
436 CD. 2018. The importance of small artificial water bodies as sources of methane emissions in
437 Queensland, Australia. Hydrol Earth Syst Sci. 22(10):5281-5298.
438 Grover SPP, Cohan A, Chan HS, Livesley SJ, Beringer J, Daly E. 2013. Occasional large
439 emissions of nitrous oxide and methane observed in stormwater biofiltration systems. Sci
440 Total Environ. 465:64-71.
441 Herrero Ortega S, Romero Gonzalez-Quijano C, Casper P, Singer GA, Gessner MO. 2019.
442 Methane emissions from contrasting urban freshwaters: Rates, drivers, and a whole-city
443 footprint. Glob Chang Biol. 25(12):4234-4243.
444 Holgerson MA, Raymond PA. 2016. Large contribution to inland water CO_2 and CH_4 emissions
445 from very small ponds. Nat Geosci. 9(3):222-226.
446 [IPCC] Intergovernmental Panel on Climate Change. 2013. Climate Change 2013: The physical
447 science basis. Contribution of working group I to the fifth assessment report of the

448 Intergovernmental Panel on Climate Change. Cambridge, United Kingdom and New York,
449 NY, USA: Cambridge University Press.
450 [IPCC] Intergovernmental Panel on Climate Change. 2019. 2019 Refinement to the 2006 IPCC
451 Guidelines for National Greenhouse Gas Inventories: Wetlands. Switzerland: IPCC.
452 Kennedy S, Sgouridis S. 2011. Rigorous classification and carbon accounting principles for low
453 and Zero Carbon Cities. Energ Policy. 39(9):5259-5268.
454 Koschorreck M, Downing AS, Hejzlar J, Marcé R, Laas A, Arndt WG, Keller PS, Smolders AJP,
455 van Dijk G, Kosten S. 2019. Hidden treasures: Human-made aquatic ecosystems harbour
456 unexplored opportunities. Ambio.
457 Marcé R, Obrador B, Gómez-Gener L, Catalán N, Koschorreck M, Arce MI, Singer G, von
458 Schiller D. 2019. Emissions from dry inland waters are a blind spot in the global carbon cycle.
459 Earth-Sci Rev. 188:240-248.
460 Marotta H, Pinho L, Gudasz C, Bastviken D, Tranvik LJ, Enrich-Prast A. 2014. Greenhouse gas
461 production in low-latitude lake sediments responds strongly to warming. Nat Clim Change.
462 4(6):467-470.
463 McAuliffe C. 1971. Gas chromatographic determination of solutes by multiple phase
464 equilibrium. Chem Technol. 1:46-51.
465 McPhillips L, Walter MT. 2015. Hydrologic conditions drive denitrification and greenhouse gas
466 emissions in stormwater detention basins. Ecol Eng. 85:67-75.
467 Nielsen O-K, Plejdrup MS, Winther M, Nielsen M, Gyldenkærne S, Mikkelsen MH, Albrektsen
468 R, Thomsen M, Hjelgaard KH, Fauser P et al. 2018. Denmark's National Inventory Report
469 2018: Emission Inventories 1990-2016-Submitted under the United Nations Framework

Convention on Climate Change and the Kyoto Protocol. Aarhus University, DCE – Danish Centre for Environment and Energy. 877156330X.

Peacock M, Audet J, Jordan S, Smeds J, Wallin MB. 2019. Greenhouse gas emissions from urban ponds are driven by nutrient status and hydrology. Ecosphere. 10(3):e02643.

Persson J, Wittgren HB. 2003. How hydrological and hydraulic conditions affect performance of ponds. Ecol Eng. 21(4):259-269.

Petersen SO, Hoffmann CC, Schäfer CM, Blicher-Mathiesen G, Elsgaard L, Kristensen K, Larsen SE, Torp SB, Greve MH. 2012. Annual emissions of CH_4 and N_2O, and ecosystem respiration, from eight organic soils in Western Denmark managed by agriculture. Biogeosciences. 9(1):403-422.

Pinheiro J, Bates D, DebRoy S, Sarkar D, R Development Core Team. 2012. nlme: linear and nonlinear mixed effects models. R package Version 3.1-103. http://CRAN.R-project.org/package=nlme.

R Development Core Team. 2018. R: A language and environment for statistical computing Vienna, Austria: R Foundation for Statistical Computing ISBN 3-900051-07-0. http://www.R-project.org/.

Sand-Jensen KAJ, Pedersen MF, Nielsen SL. 1992. Photosynthetic use of inorganic carbon among primary and secondary water plants in streams. Freshwat Biol. 27(2):283-293.

Sønderup MJ, Egemose S, Hansen AS, Grudinina A, Madsen MH, Flindt MR. 2016. Factors affecting retention of nutrients and organic matter in stormwater ponds. Ecohydrology. 9(5):796-806.

Sørensen J, Tiedje JM, Firestone RB. 1980. Inhibition by sulfide of nitric and nitrous oxide reduction by denitrifying Pseudomonas fluorescens. Appl Environ Microbiol. 39(1):105-108.

493 Taylor S, Gilbert PJ, Cooke DA, Deary ME, Jeffries MJ. 2019. High carbon burial rates by small
494 ponds in the landscape. Front Ecol Environ. 17(1):25-31.
495 Teurlincx S, Kuiper JJ, Hoevenaar ECM, Lurling M, Brederveld RJ, Veraart AJ, Janssen ABG,
496 Mooij WM, de Senerpont Domis LN. 2019. Towards restoring urban waters: understanding
497 the main pressures. Curr Opin Env Sust. 36:49-58.
498 Thermo Scientific. 2014. Anion determinations in municipal wastewater samples using EPA
499 method 300.1 (A) on an integrated ion chromatography system. Sunnyvale, CA, USA:
500 Thermo Scientific.
501 Tiedje JM. 1982. Denitrification. In: Page AL, editor. Methods of soil analysis Part 2. Second
502 Edition. ed. Madison, Wisconsin, USA.: American Society of Agronomy; p. 1011-1024.
503 United Nations. 2018. World urbanization prospects: the 2018 revision. New York: United
504 Nations, Department of Economic and Social Affairs, Population Division.
505 van Bergen TJHM, Barros N, Mendonça R, Aben RCH, Althuizen IHJ, Huszar V, Lamers LPM,
506 Lürling M, Roland F, Kosten S. 2019. Seasonal and diel variation in greenhouse gas
507 emissions from an urban pond and its major drivers. Limnol Oceanogr. 64(5):2129-2139.
508 Wanninkhof R. 1992. Relationship between wind-speed and gas-exchange over the ocean. J
509 Geophys Res-Oceans. 97(C5):7373-7382.
510 Weiss RF. 1974. Carbon dioxide in water and seawater: the solubility of a non-ideal gas. Mar
511 Chem. 2(3):203-215.
512 Weiss RF, Price BA. 1980. Nitrous-oxide solubility in water and seawater. Mar Chem. 8(4):347-
513 359.
514 Wiesenburg DA, Guinasso NL. 1979. Equilibrium solubilities of methane, carbon monoxide, and
515 hydrogen in water and sea water. Journal of Chemical & Engineering Data. 24(4):356-360.

516 Zhou Y, Zhou L, Zhang Y, Garcia de Souza J, Podgorski DC, Spencer RGM, Jeppesen E,
517 Davidson TA. 2019. Autochthonous dissolved organic matter potentially fuels methane
518 ebullition from experimental lakes. Water Res. 166:115048.
519 Zuur AF, Ieno EN, Walker N, Saveliev AA, Smith GM. 2009. Mixed effects models and
520 extensions in ecology with R. New York: Springer. (Statistics for Biology and Health).
521

Table 1. Characteristics of the water samples collected in urban ponds in four different sampling periods.

Parameters	units	Sampling period																								
		August 2018					November 2018					March 2019					June 2019					All four sampling periods				
		mean	±sd	min	max	*n*	mean	±sd	min	max	*n*	mean	±sd	min	max	*n*	mean	±sd	min	max	*n*	mean	±sd	min	max	*n*
Water temperature	°C	17.8	1.0	15.0	19.2	37	4.6	1.7	1.9	9.2	36	5.2	0.6	4.3	7.0	37	20.0	3.6	12.1	26.9	36	11.9	7.3	1.9	26.9	146
pH		7.5	0.7	5.1	9.5	37	7.5	0.3	6.9	8.3	36	7.5	0.2	6.9	7.9	37	8.0	0.7	7.3	9.8	36	7.6	0.6	5.1	9.8	146
Oxygen	mg L^{-1}	7.2	1.9	2.7	11.1	37	10.9	2.3	5.9	13.1	36	11.1	1.6	6.7	14.0	37	8.6	1.9	5.5	14.2	36	9.4	2.5	2.7	14.2	146
Oxygen saturation	%	74	23	9	120	37	86	19	46	111	36	88	12	55	112	37	91	25	12	156	36	85	21	9	156	146
Total nitrogen	mg N L^{-1}	1.1	0.6	0.5	3.0	37	1.2	1.0	0.1	4.9	36	1.1	0.3	0.3	2.0	37	0.9	0.4	0.3	2.1	36	1.07	0.6	0.1	4.9	146
Nitrate	mg N L^{-1}	0.4	0.3	0.0	1.4	37	0.4	0.4	0.0	1.8	36	0.5	0.3	0.0	1.6	37	0.2	0.3	0.0	1.3	36	0.35	0.4	0.0	1.8	146
Ammonium	mg N L^{-1}	0.2	0.2	0.0	0.7	37	0.2	0.3	0.0	1.1	36	0.1	0.0	0.0	0.2	37	0.1	0.1	0.0	0.7	36	0.12	0.2	0.0	1.1	146
Total phosphorus	mg P L^{-1}	0.15	0.17	0.02	0.78	37	0.14	0.22	0.00	0.85	36	0.08	0.08	0.01	0.43	37	0.18	0.24	0.02	1.24	36	0.19	0.19	0.00	1.24	146
Phosphate	mg P L^{-1}	0.02	0.04	0.00	0.23	37	0.02	0.04	0.00	0.22	36	0.01	0.02	0.00	0.10	37	0.02	0.06	0.00	0.36	36	0.02	0.04	0.00	0.36	146
Total organic carbon	mg L^{-1}	9.8	10.6	1.9	45.4	37	7.5	6.7	2.0	35.8	36	6.2	5.4	0.1	24.3	37	9.5	6.7	3.1	37.2	36	8.2	7.7	0.1	45.4	146
Chloride	mg L^{-1}	51	136	1.8	775.8	37	54.8	47	8.3	207.8	36	53.3	46	11.2	208.4	37	43.0	39	2.4	127.2	36	50.4	78	1.8	775.8	146
Sulphate	mg L^{-1}	14	39	0.1	237.0	37	22.3	25	0.5	129.2	36	13.2	16	1.1	90.7	37	20.4	25	0.3	107.1	36	17.4	28	0.1	237.0	146
Vegetation cover	%	38	33	0	100	37	32	31	0	100	36	12	22	0	80	37	50	34	2	100	36	33	33	0	100	146
Carbon dioxide	µg C L^{-1}	1697	1535	75	8116	37	1956	1894	196	8476	36	985	924	78	3784	37	3148	3282	80	15024	36	1938	2208	75	15024	146
Methane	µg C L^{-1}	19	43	0.3	258	37	24.2	59	0.1	264	36	7.2	13	0.1	57	37	125	384	1.4	2257	36	44	1982	0.1	2257	146
Nitrous oxide	µg N L^{-1}	1.5	3.1	0.4	19.7	37	0.7	1.0	0.1	4.7	36	0.4	0.3	0.1	1.1	37	0.7	1.0	0.2	5.3	36	0.8	1.8	0.1	19.7	146

Figures

Figure 1. Daily mean air temperature (°C) and precipitation (mm) at the studied ponds. Data obtained from DMI.

Figure 2. Boxplot showing the concentrations of a) CO_2, b) CH_4, and c) N_2O in the ponds in the four sampling periods. Horizontal bold lines indicate the median, boxes the 25% and 75% percentiles, and whiskers extend to the most extreme values (minimum or maximum) provided that they are within 1.5 times the interquartile range from the top (bottom) of the box. Otherwise, the value is represented individually as points.

Figure 3. Functions fitted for 12 environmental variables by a boosted regression tree (BRT) model relating the probability of carbon dioxide (CO_2) concentrations in urban ponds to the environment. A common scale is used on the vertical axis for all plots.

Figure 4. Functions fitted for 12 environmental variables by a boosted regression tree (BRT) model relating the probability of methane (CH_4) concentrations in urban ponds to the environment. A common scale is used on the vertical axis for all plots.

Figure 5. Functions fitted for 12 environmental variables by a boosted regression tree (BRT) model relating the probability of nitrous oxide (N_2O) concentrations in urban ponds to the environment. A common scale is used on the vertical axis for all plots.

Figure 6. Plots showing the concentrations in CO_2 (a), CH_4 (b), and N_2O (c) as a function of the best explanatory variables identified in the BRT models, i.e. vegetation cover, water temperature and NO_3^- concentration, respectively. The different symbols represent the different sampling periods.

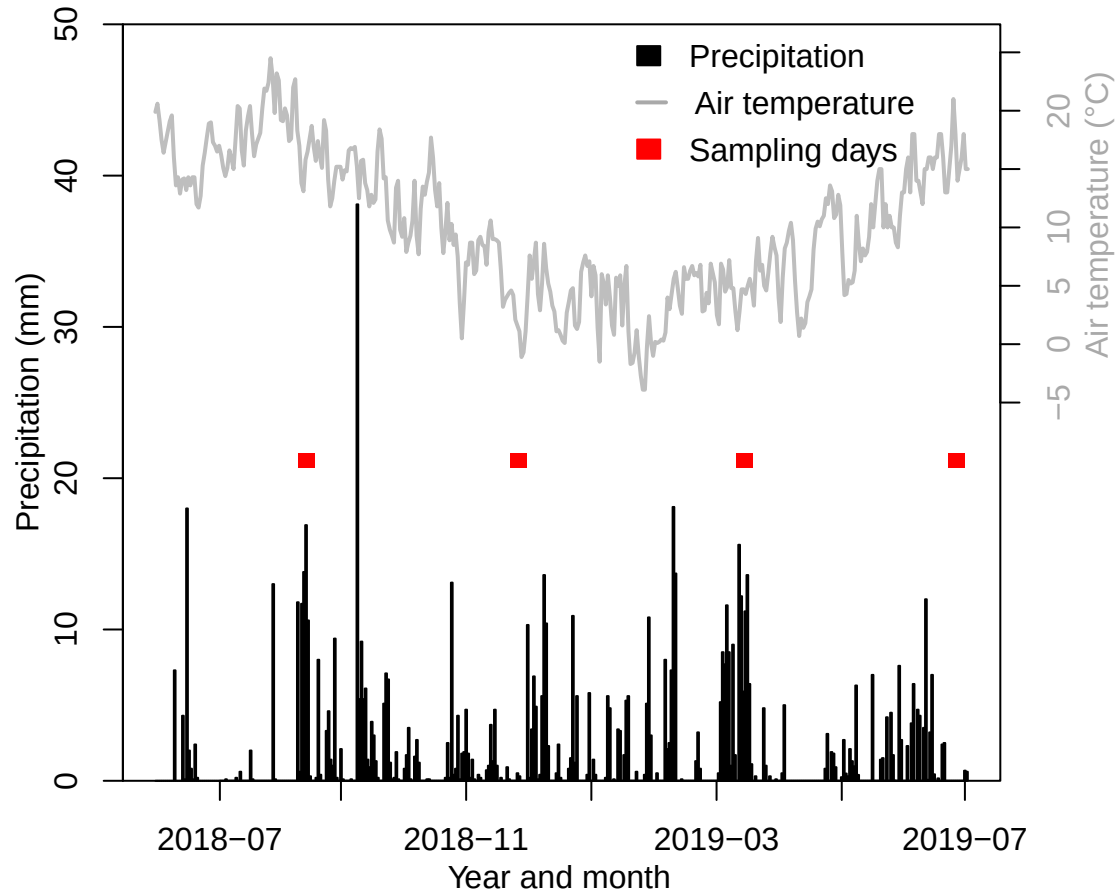
Precipitation
Air temperature
Sampling days
Precipitation (mm)
0
10
20
30
40
50
Air temperature (°C)
−5
0
5
10
20
2018−07
2018−11
2019−03
2019−07
Year and month

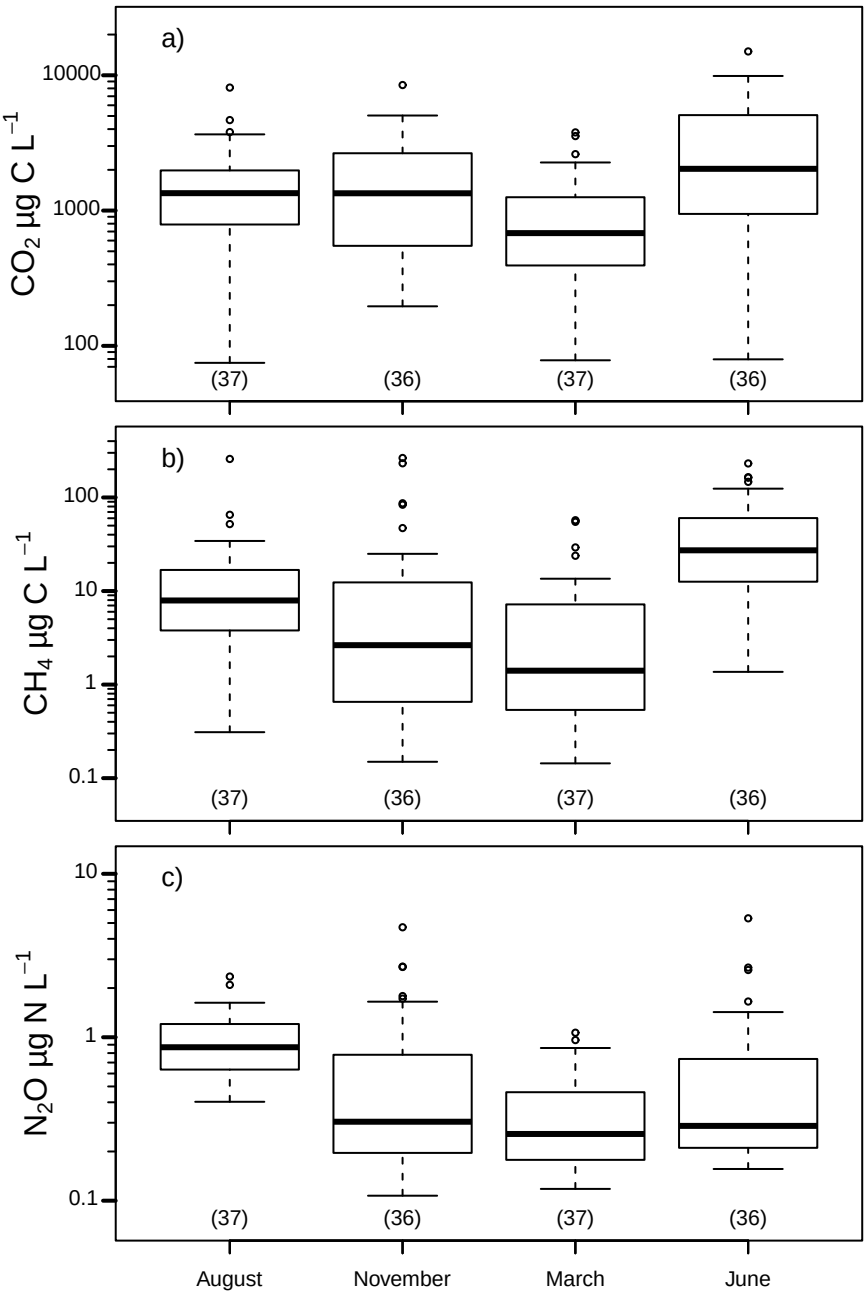
a)
10000
1000
100
CO_2 µg C L^{-1}
(37)
(36)
(37)
(36)
b)
100
10
1
0.1
CH_4 µg C L^{-1}
(37)
(36)
(37)
(36)
c)
10
1
0.1
N_2O µg N L^{-1}
(37)
(36)
(37)
(36)
August
November
March
June

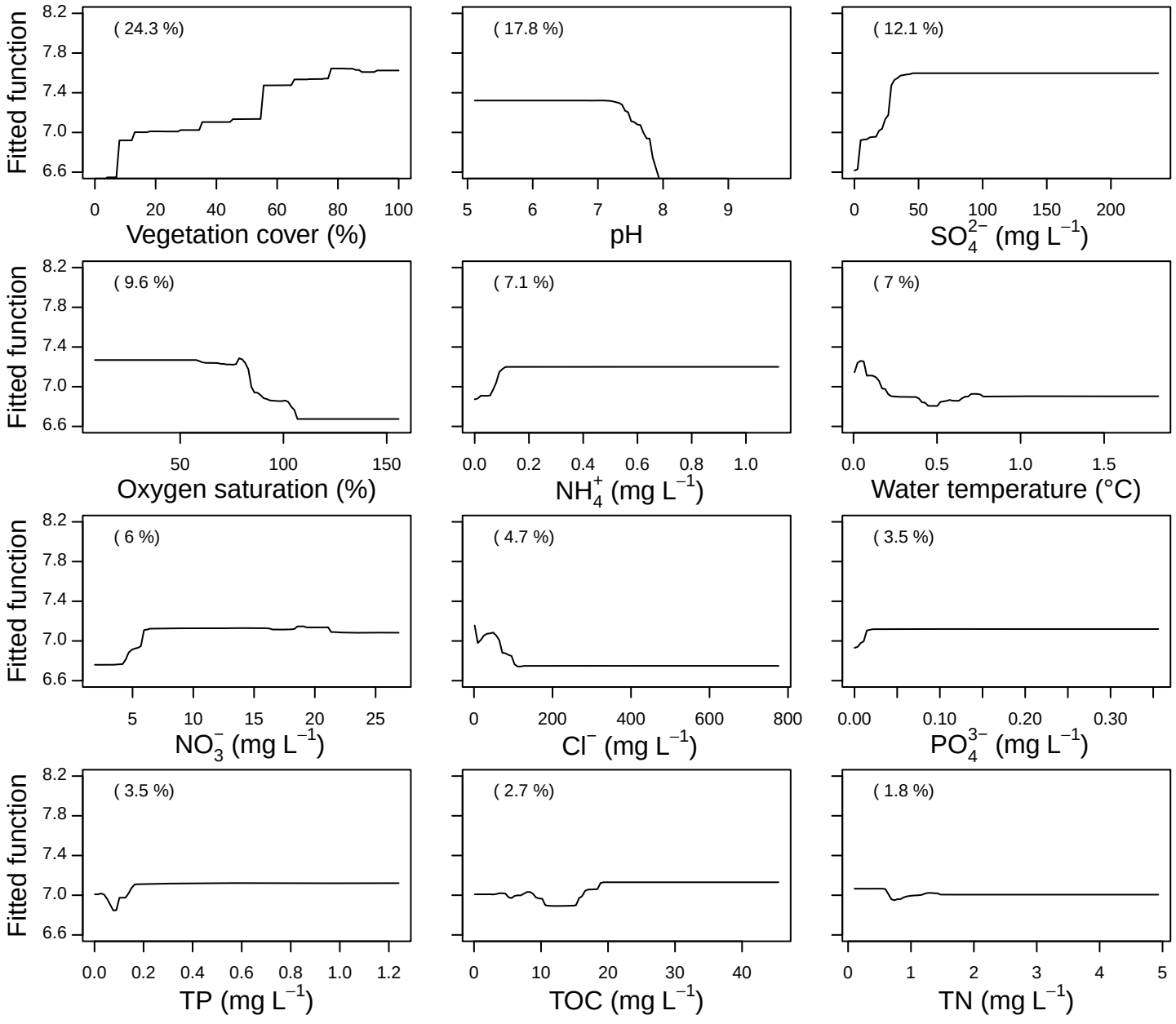
Fitted function
8.2
7.8
7.4
7.0
6.6
(24.3 %)
0
20
40
60
80
100
Vegetation cover (%)
(17.8 %)
5
6
7
8
9
pH
(12.1 %)
0
50
100
150
200
SO4 2− (mg L−1)
(9.6 %)
50
100
150
Oxygen saturation (%)
(7.1 %)
0.0
0.2
0.4
0.6
0.8
1.0
NH4 + (mg L−1)
(7 %)
0.0
0.5
1.0
1.5
Water temperature (°C)
(6 %)
5
10
15
20
25
NO3 − (mg L−1)
(4.7 %)
0
200
400
600
800
Cl− (mg L−1)
(3.5 %)
0.00
0.10
0.20
0.30
PO4 3− (mg L−1)
(3.5 %)
0.0
0.2
0.4
0.6
0.8
1.0
1.2
TP (mg L−1)
(2.7 %)
0
10
20
30
40
TOC (mg L−1)
(1.8 %)
0
1
2
3
4
5
TN (mg L−1)

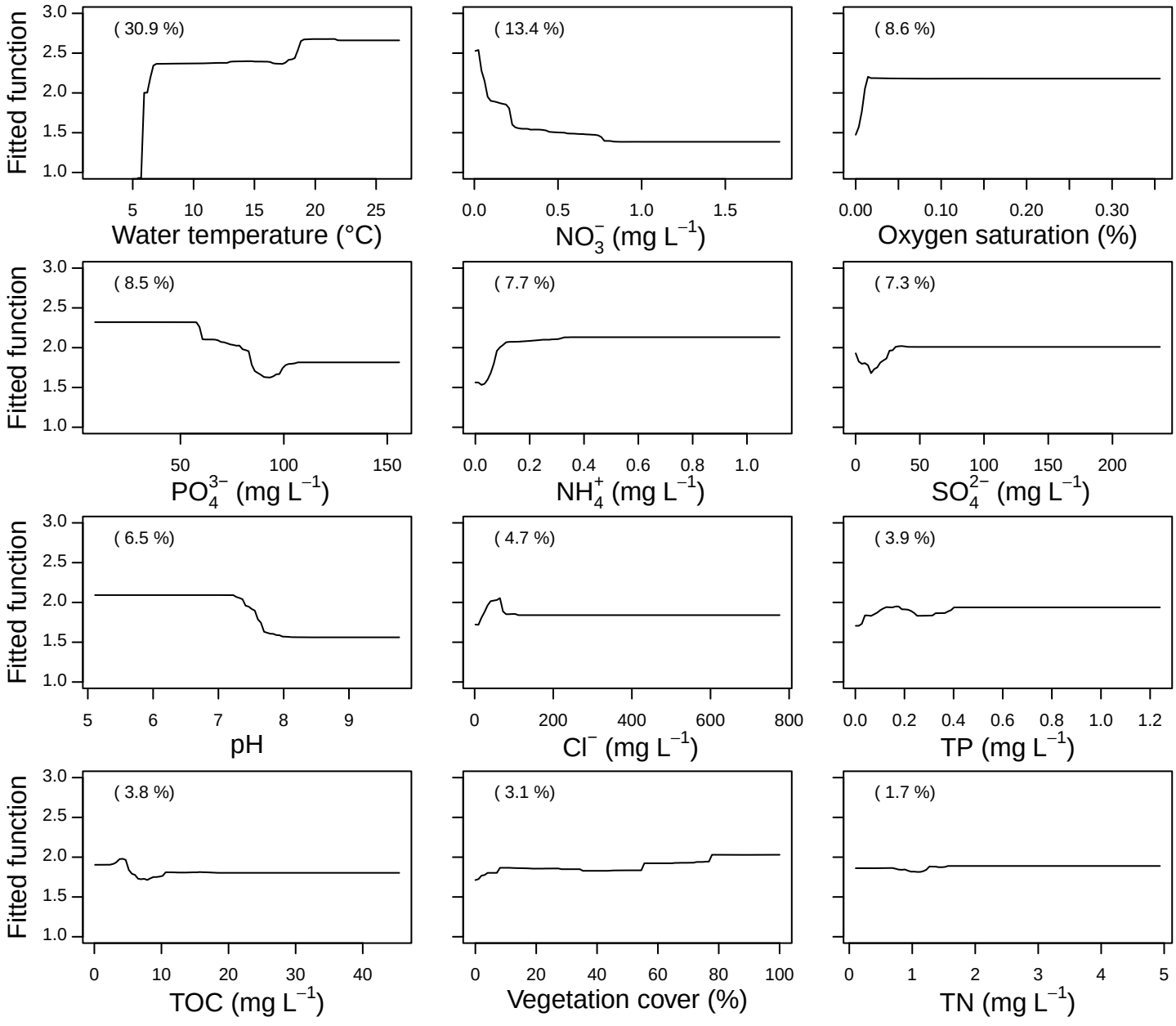
Fitted function
(30.9 %)
Water temperature (°C)
(13.4 %)
NO3− (mg L−1)
(8.6 %)
Oxygen saturation (%)
(8.5 %)
PO43− (mg L−1)
(7.7 %)
NH4+ (mg L−1)
(7.3 %)
SO42− (mg L−1)
(6.5 %)
pH
(4.7 %)
Cl− (mg L−1)
(3.9 %)
TP (mg L−1)
(3.8 %)
TOC (mg L−1)
(3.1 %)
Vegetation cover (%)
(1.7 %)
TN (mg L−1)

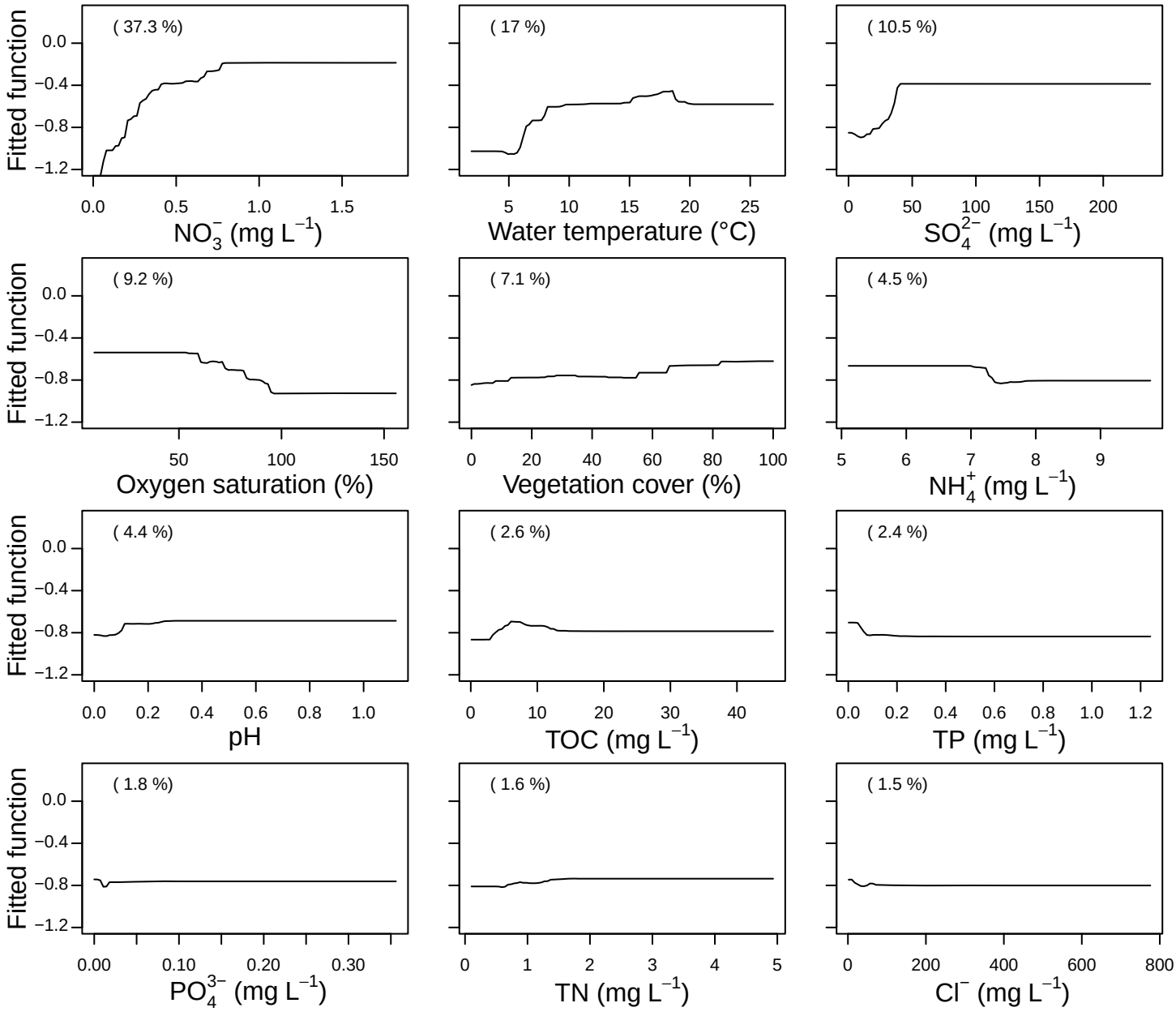
Fitted function
(37.3 %)
(17 %)
(10.5 %)
(9.2 %)
(7.1 %)
(4.5 %)
(4.4 %)
(2.6 %)
(2.4 %)
(1.8 %)
(1.6 %)
(1.5 %)
NO_3^- (mg L^{-1})
Water temperature (°C)
SO_4^{2-} (mg L^{-1})
Oxygen saturation (%)
Vegetation cover (%)
NH_4^+ (mg L^{-1})
pH
TOC (mg L^{-1})
TP (mg L^{-1})
PO_4^{3-} (mg L^{-1})
TN (mg L^{-1})
Cl^- (mg L^{-1})

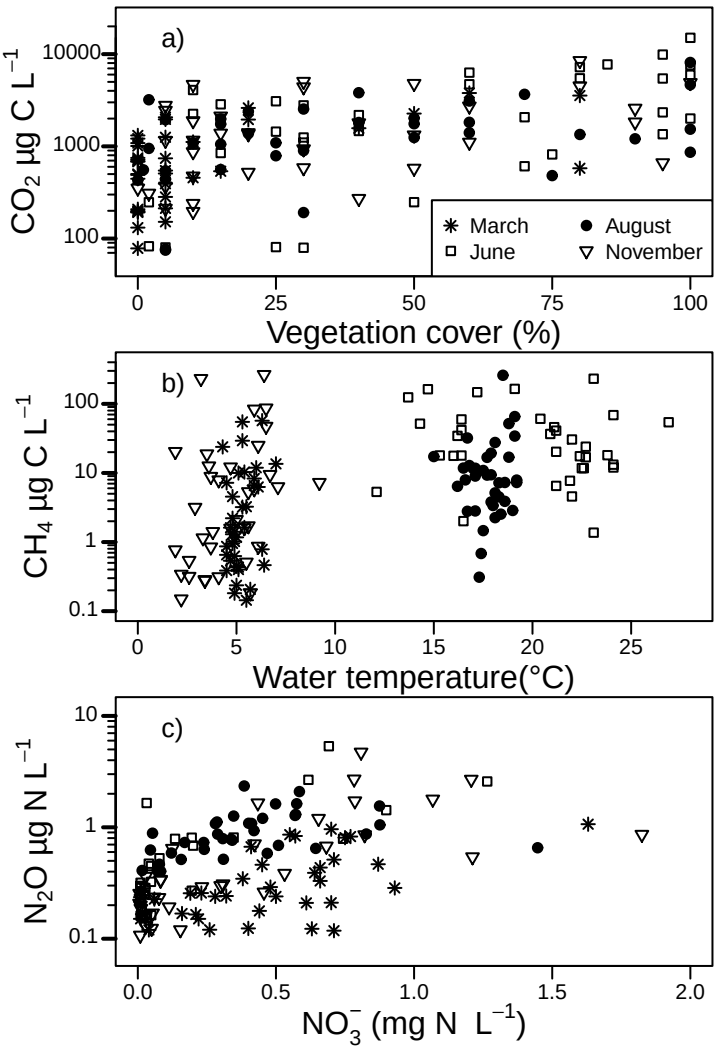
a)
CO_2 µg C L^{-1}
10000
1000
100
0
25
50
75
100
Vegetation cover (%)
March
August
June
November
b)
CH_4 µg C L^{-1}
100
10
1
0.1
0
5
10
15
20
25
Water temperature(°C)
c)
N_2O µg N L^{-1}
10
1
0.1
0.0
0.5
1.0
1.5
2.0
NO_3^- (mg N L^{-1})